

Observations of droplet impingement on a ceramic porous surface

S. CHANDRA

Department of Mechanical Engineering, University of Toronto, Toronto, Ontario M5S 1A4, Canada

and

C. T. AVEDISIAN

Sibley School of Mechanical and Aerospace Engineering, Cornell University, Ithaca, NY 14853-7501, U.S.A.

(Received 30 May 1991 and in final form 5 November 1991)

Abstract—The dynamic aspects of droplet impingement on a porous ceramic surface were studied experimentally. Single-shot flash photography was used to photographically record the deformation and spreading on the surface. The observations were made with ambient pressure (0.10 MPa), ambient temperature (*ca.* 22°C), initial droplet diameter (1.5 mm), and the impact Weber number (43) fixed. The primary parameter was the surface temperature, which ranged from 22 to 200°C. The liquid was *n*-heptane. The spreading rate of a droplet on a porous surface at 22°C was measured to be lower than that on a stainless steel surface. No transition to film boiling was observed with the porous surface at a surface temperature of 200°C, unlike that seen with a stainless steel surface. The evolution of wetted area and spreading rate, both of a droplet on a porous surface as well as on a stainless steel surface, were found to be independent of surface temperature during the early period of impact. This result was attributed to negligible surface tension and viscous effects. The maximum value of the diameter of liquid which spreads on the surface was found to be lower on the ceramic surface than it was on the stainless steel surface at the same temperature.

1. INTRODUCTION

THE IMPACT of a liquid droplet on a hot surface has been studied extensively because of its significance in a wide variety of applications. Prior experimental studies [1-10] were specifically concerned with the collision and deformation processes of droplets hitting a *non-porous* surface. A few studies have considered experimentally the evaporation of very softly deposited droplets on *porous* surfaces—droplets which experienced minimal deformation on impact—with the emphasis being on the droplet evaporation process [11]. One prior study has reported results for droplets impacting on porous surfaces [12], but the photographs of the impact process showed few clear details.

The importance of the problem of droplet impingement on porous surfaces stems from its relevance to fire suppression using sprinkler systems; droplet impingement cooling of ceramic-encased semiconductor chips; and the burning of combustible liquid sprays during which the droplets within the spray may impact the combustor wall (e.g. ceramic-lined walls of an incinerator). An understanding of the droplet impact process on porous surfaces is particularly important in fire suppression because fires generally involve burning porous materials (e.g. wood), and one of the most important processes that influence fire suppression using sprinklers may be the splash

dynamics of droplets of the suppressant liquid on the burning surface and the attendant influences these dynamics have on heat transfer to the surface.

The present paper reports results of an experimental study of the collision and deformation dynamics of droplets impacting on a porous surface. The objectives were to: (1) photograph the impact of a droplet on a porous surface for several different values of the surface temperature (2) measure the evolution of droplet shape during impact (e.g. spreading diameter and droplet height), and (3) compare the results with measurements made during experiments on droplet impact on a stainless steel surface, and also to relevant analyses. The experimental method centered on using a flash-photographic method to record details of the impact process. The liquid studied was *n*-heptane (C_7H_{16}). The initial droplet diameter was 1.50 mm and the droplet velocity at the time of impact was 0.93 m s^{-1} , corresponding to an impact Reynolds number (*Re*) of 2300 and Weber number (*We*) of 43. The ambient pressure (0.101 MPa), and ambient temperature (*ca.* 22°C), were held constant.

The collision dynamics of a droplet with a porous surface, and the subsequent spreading and evaporation of the droplet, may be different than on a non-porous surface because of the effect of surface roughness and/or the potential for liquid to seep into the porous surface during the deformation and spreading process. Liquid seepage may influence the

NOMENCLATURE

c	specific heat	T_w	solid surface temperature
d	diameter of wetted area	W	energy to deform droplet during impact
d_{\max}	maximum diameter of wetted area	We	$\equiv \rho_1 U^2 D / \sigma$
D	droplet diameter before impact	Greek symbols	
E_{ki}	kinetic energy ($i = 1$ before impact ; $i = 2$ after impact and spreading)	α	angle of inclination of the camera to the horizontal
E_{si}	surface energy ($i = 1$ before impact ; $i = 2$ after impact and spreading)	β	spread factor ($\equiv d/D$)
E_p	energy lost due to liquid penetration into the ceramic surface	ζ	dimensionless droplet height ($\equiv h/D$)
h	droplet height above surface	θ	apparent contact angle
k	thermal conductivity	κ	$\equiv 1/k\rho c$
Re	$\equiv \rho_1 UD / \mu_1$	μ	viscosity
t	time	ρ	density
t_e	droplet evaporation time	σ	surface tension.
T_c	liquid critical temperature	Subscripts	
T_i	droplet temperature before impact	l	liquid
$T_{L,p}$	Leidenfrost temperature on a porous, ceramic surface	p	porous ceramic surface
$T_{L,ss}$	Leidenfrost temperature on stainless steel	s	solid
		ss	stainless steel surface.

spreading rate, the size of the effective wetted area covered by the advancing film, and also the transition to film boiling (defined by the so-called 'Leidenfrost' temperature) by its effect on maintaining liquid-solid contact as the surface temperature is increased. Surface roughness can increase the effective area for heat transfer between the surface and the droplet, thereby increasing the heat transfer, and thus the liquid evaporation rate.

The droplet impact dynamics depend on the impact energy of the droplet, the temperature of the surface, and the surface porosity. Depending on the impact energy, a measure of which is the Weber number, the droplet may shatter during the deformation process, it may spread into a thin liquid film, it may rebound, or it may penetrate the surface (in the case of a porous surface). The present work examines the effect of surface temperature and surface porosity on the impact dynamics with the initial impact energy fixed at a value ($We = 43$) for which the droplet did not shatter (but still deformed and spread along the surface) upon impact, allowing measurements to be made of the droplet shape during its spreading on the porous surface.

A single-shot flash photographic method was used to record the evolution of the droplet shape during impact. A single photograph was taken at one instant during the impact process for each drop studied. The assumption is that the impact process is sufficiently repeatable from drop to drop that by photographing successive stages of the impact for several different drops the evolution of the droplet dynamics can be pieced together from individual images of droplets taken at progressive stages during impact [13]. An

advantage of this method is that the effective exposure time of each image is equal to the duration of the flash ($\sim 0.5 \mu\text{s}$), which is short enough to effectively eliminate any blurring due to the motion of the droplet.

The porous surface studied in this work was made of a machinable alumina (Al_2O_3) ceramic of approximately 25% porosity. The ceramic consisted of closely packed alumina particles with a nominal size of approximately 5 to 10 μm . Further details of the surface structure are given elsewhere [11] (in which it is referred to as the 'P2' surface). The surface temperature was varied from 22 to 200°C. This range included the liquid boiling point (98.4°C) and the Leidenfrost temperature for *n*-heptane on a stainless steel surface (200°C [10]) so that droplets both wetting the surface and levitated above it were studied.

2. DESCRIPTION OF THE EXPERIMENTAL APPARATUS

A schematic diagram of the experimental apparatus is shown in Fig. 1. It consisted of (1) a syringe pump and hypodermic needle to form and release the drop, (2) the test surface on which the droplet fell, (3) a 35 mm camera, (4) a flash unit to provide illumination for photography, and (5) an optical interruptor and time delay circuit to detect the release of the droplet and trigger the flash. Details of the apparatus are described elsewhere [13]. A brief description is given below.

Droplets were formed by forcing liquid from a Sage Instruments model 341A syringe pump at a flow rate of 0.69 ml min⁻¹ through a stainless steel hypodermic

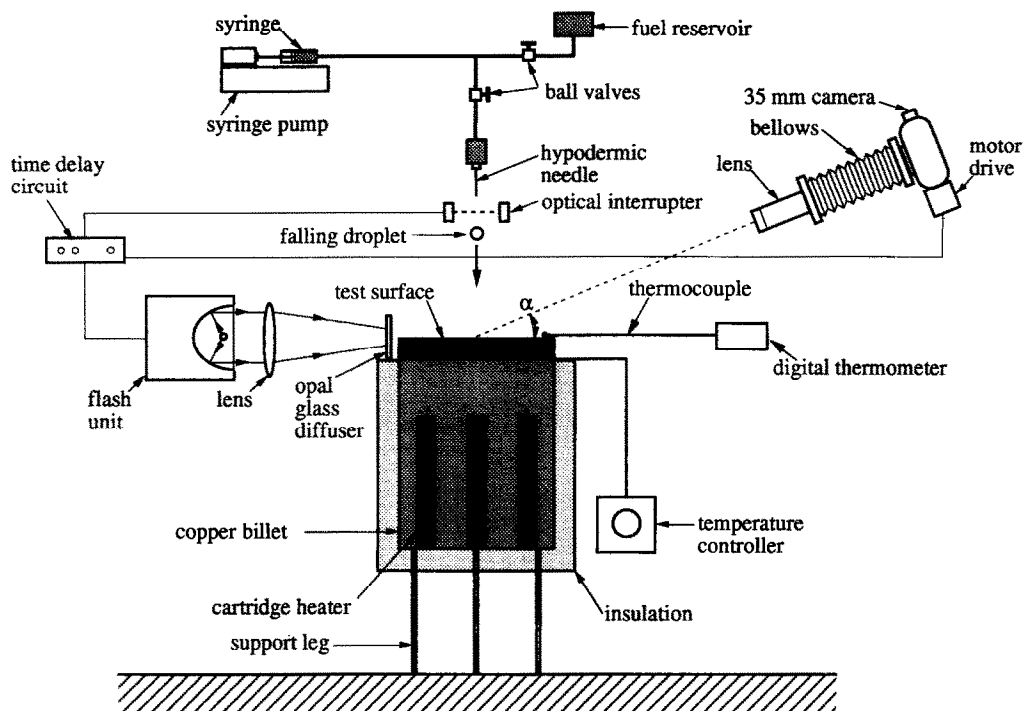


FIG. 1. Schematic of the apparatus.

needle. The flow rate was low enough to allow a droplet to form at the needle tip and detach under its own weight. The release of the droplet was detected by placing an optical interrupter approximately 5 mm below the tip of the needle. The passage of a drop through the light beam of the optical interrupter sent a signal to a time delay unit which opened the camera shutter. After a preset time interval the flash unit (an E.G.&G. 549-11 unit that provided a $0.5 \mu\text{s}$ duration flash) was triggered to take a single photograph of the drop impacting the test surface. The intensity of the flash was so much greater than that of the ambient light that the film was effectively exposed only by the light of the flash, even though the shutter was actually opened for $1/8 \text{ s}$.

The test surfaces were 64 mm in diameter and 3.2 mm thick. They were heated by placing them on a cylindrical copper billet containing five symmetrically placed cartridge heaters (Hotwatt HS374). The surface temperature of the porous ceramic surface was measured by cementing the beads of two chromel-alumel thermocouples to the upper face of the surface, at diametrically opposed positions midway between the center and edge of the surface. When the surface temperature reached steady state the readings from these two thermocouples were within 1°C of each other.

A Nikon F-3 camera equipped with a 105 mm f-4 lens, extension bellows, and motor drive was used to take the photographs. The camera was aligned at an angle α to the horizontal which was fixed at 0° . Not

enough light was reflected from the porous surface to allow good quality (perspective) photographs to be taken when the camera was positioned at $\alpha \neq 0^\circ$. By contrast, a metallic surface readily reflects light thus allowing clear perspective droplet images to be obtained when non-zero values of α are used [10]. The lens aperture was stopped down to f-22 to provide adequate depth of field. The film used was Kodak TMAX 400, push processed to 1600 ASA by developing for 8 min in Kodak TMAX developer at 24°C .

Droplet dimensions were measured directly from 35 mm negatives by placing the film in a photographic enlarger and then projecting the image onto a screen. A scale factor was determined from an image of 4.763 mm diameter stainless steel dowel. The resolution of measurements made from the projected image using dividers and a steel scale was $\pm 0.5 \text{ mm}$, which translates into an accuracy of droplet diameter measurement of $\pm 0.01 \text{ mm}$.

Droplet evaporation times were measured by recording the droplet evaporation using a Video Logic CDR 460 video camera. A time display with a resolution of 0.1 s was added to the video image by a Vicon V240TW timer. The droplet evaporation time was defined as the interval between droplet impact and the instant when the droplet could no longer be seen. In the case of droplets evaporating on a porous surface, though, this method could lead to some ambiguity in the definition of the droplet evaporation time, because liquid was simultaneously evaporated and absorbed by the surface.

3. DISCUSSION

The impact of a drop of *n*-heptane on a porous surface at 22 °C is illustrated by the sequence of photographs shown in Fig. 2. A period of 2.6 ms is shown during which time the droplet assumed the shape of

a flattened disk (the liquid continued to spread after this time, reaching a maximum diameter of 5.01 mm at $t \approx 20$ ms). The upper half of the droplet appears to be darker than the lower half because the edge of the porous surface is reflected in the droplet which acts as a convex lens to invert the image.

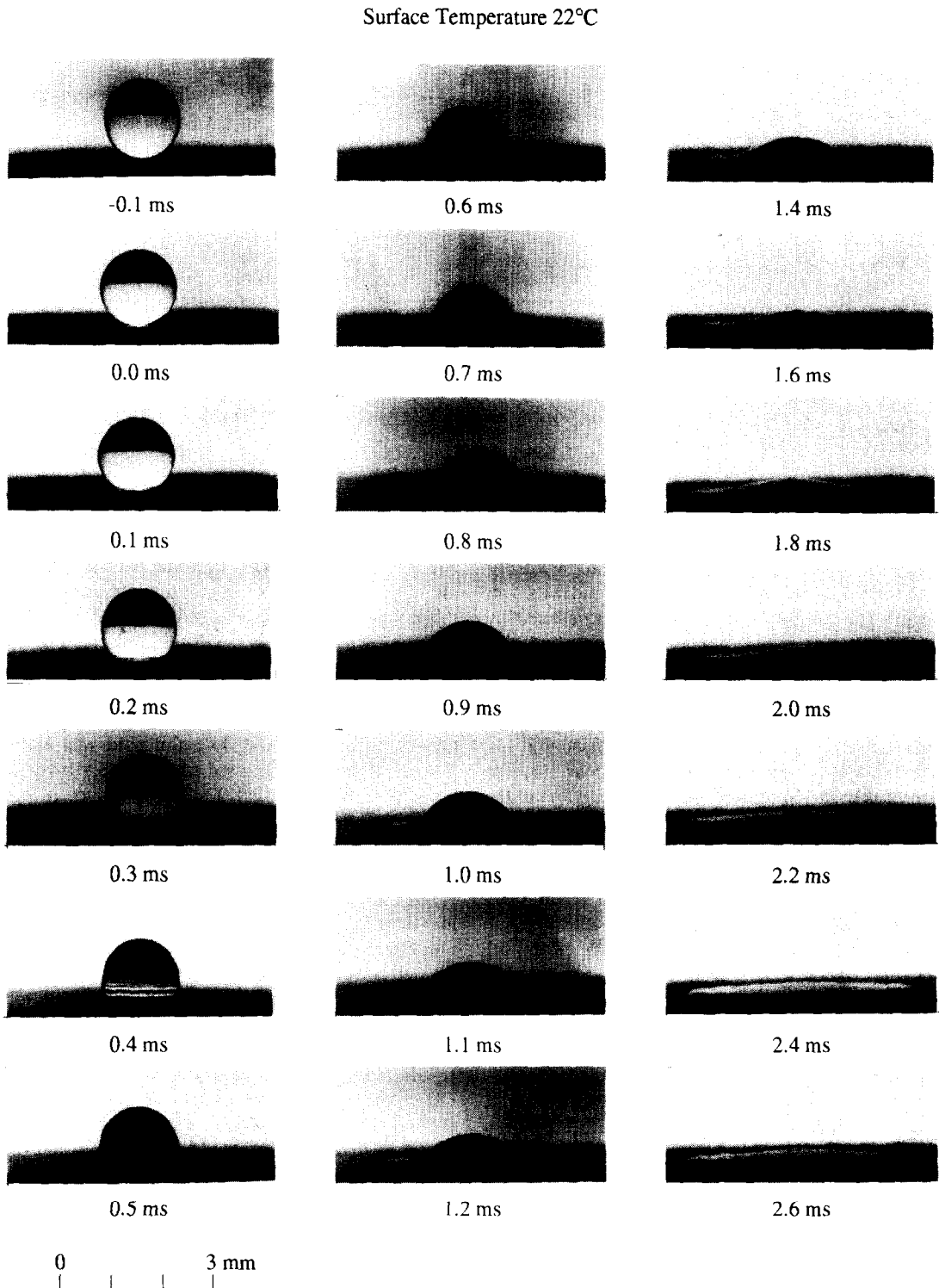


FIG. 2. The impact of a *n*-heptane droplet on the ceramic surface at 22 °C.

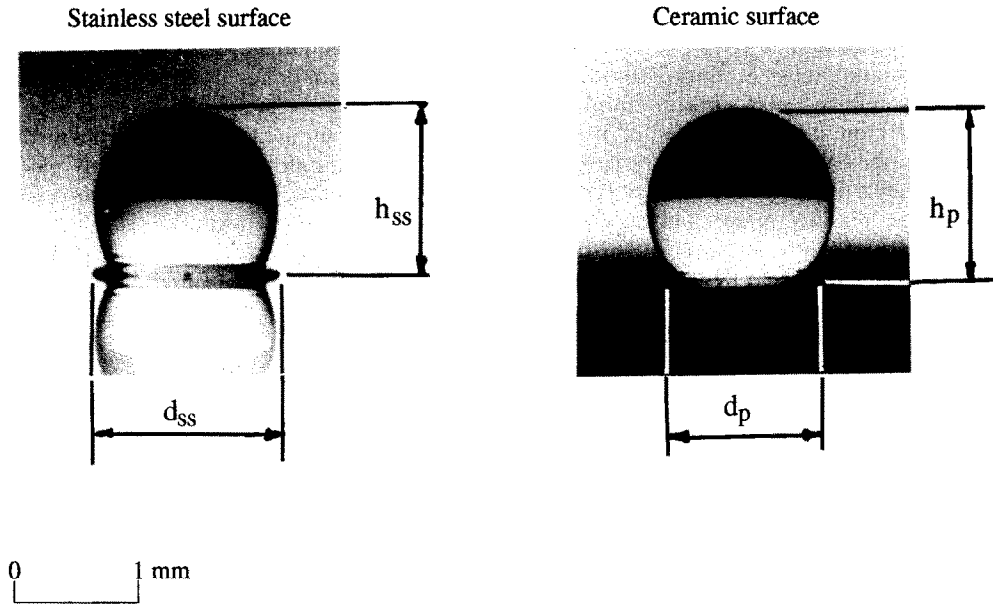


FIG. 3. Droplet impact on (a) a stainless steel surface and (b) a ceramic surface, 0.2 ms after impact ($T_w = 22^\circ\text{C}$). The wetted diameter (d) is seen to be greater on the stainless steel surface than it is on the ceramic surface. No difference could be measured between the values of the droplet height (h) for the two surfaces.

Liquid jets out sideways from beneath the droplet away from the point of impact, starting at approximately 0.3 ms after impact. This sideways jetting is similar to that which has been observed on a stainless steel surface. The jetting is caused by the rapid pressure increase in the drop at the point of impact. The pressure is relieved by the motion of the liquid along the surface through formation of the jet at the base of the droplet. The jet appears to form later than for impact on a stainless steel surface, where it was observed within the first 0.1 ms after impact [10].

Figure 3 compares enlarged views of a droplet impacting on a stainless steel surface with a droplet on the ceramic surface, taken 0.2 ms after impact in both cases. The visible diameter of the wetted area is indicated, as is the height of the droplet above the surface. The diameter of the wetted area on the ceramic surface is smaller than on the stainless steel surface. The difference could be due to the fact that the pressure in the liquid at the point of impact can drive some of the liquid into the porous surface, rather than just sideways, as is the case when the surface is impermeable.

Increasing the surface temperature can significantly alter the droplet impact dynamics. One method of identifying the values of surface temperature at which changes occur in the impact, spreading, and evaporation process (e.g. a transition from nucleate to film boiling) is to plot a curve of the droplet lifetime (t_e) as a function of the surface temperature (T_w) [14]. Such curves are shown in Fig. 4 for droplets of *n*-heptane (with an initial diameter of 1.5 mm) evaporating on both the steel and ceramic surfaces. The form of the curve is the same for both surfaces except

that the evaporation time is lower on the ceramic surface than the steel surface, and that wetting on the ceramic surface persists to higher temperatures than on the steel surface. Above about 200°C , which is approximately the Leidenfrost temperature for heptane on stainless steel ($T_{L,ss}$ in Fig. 4), the droplet still wets the ceramic surface. This difference in surface wetting accounts for the large differences in evaporation times at temperatures higher than 200°C because direct contact heat transfer across the solid-liquid interface is higher than across the vapor gap

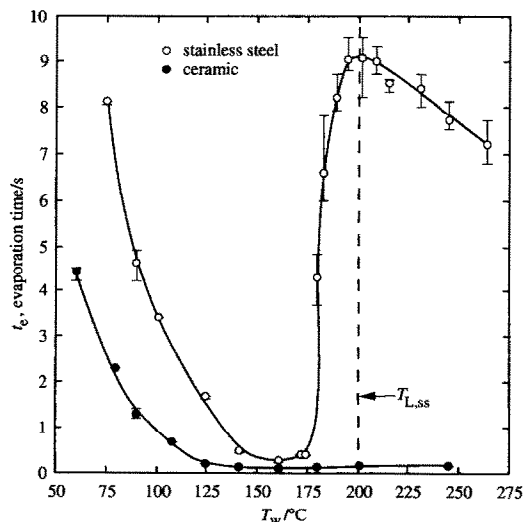


FIG. 4. Leidenfrost curve for droplets of *n*-heptane (1.5 mm initial diameter) on a stainless steel surface.

that separates the droplet from the surface above the Leidenfrost temperature.

For the temperature range in which wetting occurs on both the ceramic and steel surfaces, droplet lifetimes are shorter on the ceramic surface than the stainless steel surface. While the reason for this fact is not precisely known, it may be the result of (1) liquid seeping into the porous surface and experiencing increased heat transfer because of the larger surface area in contact with the liquid by the porous matrix or (2) increased heat transfer to the drop at the liquid–solid interface due to an increased surface area of the ceramic surface (due to roughness) than the smooth steel surface. Also, if liquid enters the surface, it is no longer visible and this fact can create the illusion of complete evaporation that would yield reduced estimates of the evaporation time.

Figure 5 shows droplets impacting on the ceramic surface at three values of T_w , which illustrate the impact dynamics in the regimes shown in Fig. 4. At $T_w = 100^\circ\text{C}$, the surface temperature is 2°C above the boiling point of *n*-heptane and vapor bubbles can be seen at the liquid–solid interface. At $T_w = 150^\circ\text{C}$ vigorous bubbling exists within the liquid. When T_w is raised to 200°C , a combination of surface wetting and levitation occurs. The droplet rebounds upon impact and does not spread out as a thin film (cf. $t = 15$ ms). Visible near the base of the droplet are waves (cf. $t = 0.3$ ms), created by the shock of the impact, propagating back into the bulk of the liquid. It is also evident that the advancing liquid film near the contact line [15], if it exists in the systems studied, is not visible (cf. $T_w = 100^\circ\text{C}$, $t = 2$ ms) with the present optical set-up.

The observations shown in Fig. 5 for $T_w = 200^\circ\text{C}$ —the approximate Leidenfrost temperature on a stainless steel surface ($T_{L,ss}$)—are to be contrasted with a droplet impacting a steel surface. In the latter case, the wetting behavior shown in Fig. 5 does not occur [10]. Rather, the droplet is levitated above the surface. Figure 6 further illustrates this difference in wetting on the stainless steel and ceramic surfaces at $T_{L,ss}$. The impingement process on the steel surface suggests that the droplet is sliding along the surface as it would were it separated from the surface by a vapor layer. The failure of the droplet to completely levitate on the ceramic surface is evident. Rather, the droplet seems to ‘stick’ to the ceramic surface, suggesting that the droplet is wetting it (power limitations prevented raising the ceramic surface temperature to a high enough value to force levitation; the highest attainable surface temperature was about 300°C with the cartridge heaters used in the copper billet). The Leidenfrost temperature is thus dependent on surface porosity/roughness, which is consistent with previous observations for methanol droplets on this ceramic surface where the Leidenfrost temperature of methanol was measured to be 202°C higher than on a stainless steel surface [11]. Two possible reasons for the Leidenfrost temperature being higher on the cer-

amic surface than on the stainless steel surface are (1) differences in the surface thermal properties, or (2) the influence of vapor or liquid seeping or being absorbed into the surface.

The effect of surface thermal properties on the Leidenfrost temperature of a droplet gently placed (i.e. $We \rightarrow 0$) on a hot *non-porous* surface has been shown empirically to be of the form [14]

$$T_{L,ss} = \frac{\frac{27}{32} T_c - T_i}{\exp(0.00175\kappa) \operatorname{erfc}(0.042\sqrt{\kappa})} + T_i \quad (1)$$

with

$$\kappa = \left(\frac{1}{k_s \rho_s C_s} \right) [\text{s cm}^4 \text{ } ^\circ\text{C}^2 \text{ cal}^{-2}]. \quad (2)$$

If no vapor penetration in the ceramic surface were to occur, or if the ceramic surface were impermeable, (1) would provide an estimate of the Leidenfrost temperature for heptane on the ceramic surface ($T_{L,p}$). Using the thermal properties of alumina, $T_{L,p}$ is predicted to be only 7°C higher than $T_{L,ss}$ (205°C from (1), which is in close agreement with the measured value of 200°C (Fig. 4)), whereas the droplet did not levitate on the ceramic surface even when T_w was increased to almost 250°C . The effect of surface thermal properties thus cannot alone explain the substantial increase in Leidenfrost temperature observed for the ceramic surface. Vapor penetration must exert some influence on the Leidenfrost temperature.

An explanation for the influence of vapor penetration into the surface is complicated and related analyses [11, 16] are not capable of specifically addressing the influence of surface porosity on the Leidenfrost temperature. The following explanation is, therefore, qualitative. We consider a surface which is impermeable and at the Leidenfrost temperature and examine the effect of progressively increasing the porosity and the attendant changes in surface temperature that are required to maintain levitation. As the surface becomes porous, vapor generated by liquid evaporation may flow into the surface as well as escape radially outward in the vapor gap between the surface and the underside of the droplet. This mass loss into the surface reduces the pressure in the vapor gap below the droplet, thereby decreasing the force which levitates the droplet above the surface. To compensate, the surface temperature must increase to increase the evaporation rate; hence the increase in the Leidenfrost temperature. More data on Leidenfrost temperature and surface porosity are required to determine the precise functional dependence of (1) on porosity, and to provide additional insights into the mechanisms that are responsible for the observed increase in Leidenfrost temperature on porous surfaces.

To quantify the droplet spreading process, two dimensions are used: the (visible) diameter of the wetted area (d), and the droplet height above the surface (h) (Fig. 7). Figure 3 further illustrates how these dimensions were actually obtained from the

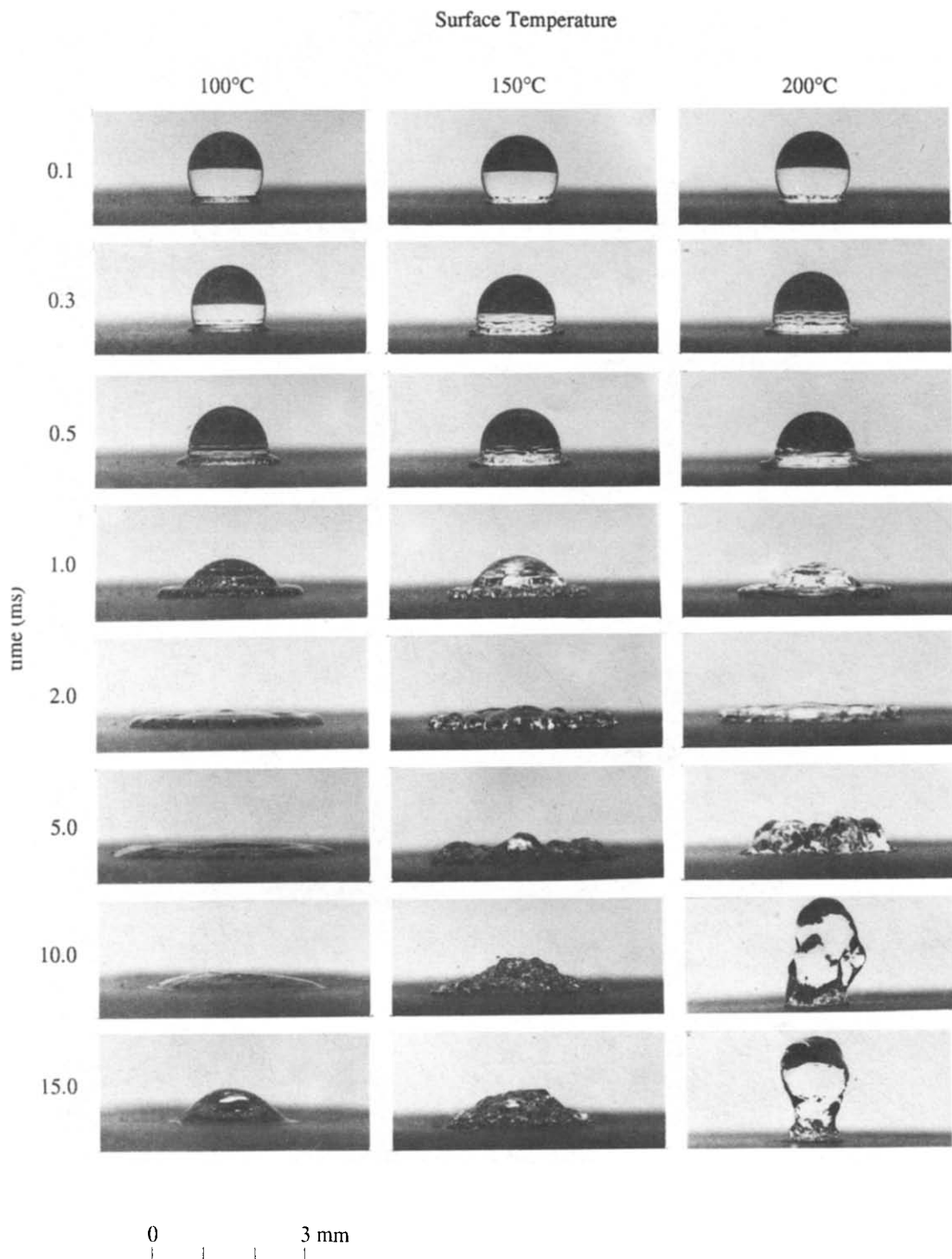


Fig. 5. The impact of an *n*-heptane droplet on a heated ceramic surface above the boiling point (98.4°C) of the liquid, with (a) $T_w = 100^\circ\text{C}$, (b) $T_w = 150^\circ\text{C}$, and (c) $T_w = 200^\circ\text{C}$.

photographic negatives. Normalizing d and h by the initial droplet diameter (D) yields the so-called 'spread factor' $\beta(t) \equiv d(t)/D$ [17] and the dimensionless height $\zeta(t) \equiv h(t)/D$. The definition of β is unambiguous when $T_w < T_{L,ss}$. When $T_w \geq T_{L,ss}$, the droplet no longer wets the surface (e.g. for the stainless steel

surface with $T_w = 200^\circ\text{C}$). $d(t)$ was then defined as the diameter of the flattened area at the bottom of the drop (Fig. 7(b)) which was separated from the solid surface by a thin vapor film during deformation. If the droplet recoils from the surface (Figs. 7(c) and (d)) when $T_w \geq T_{L,ss}$ d can approach zero (Fig. 7(d)). Our

Surface Temperature 200°C

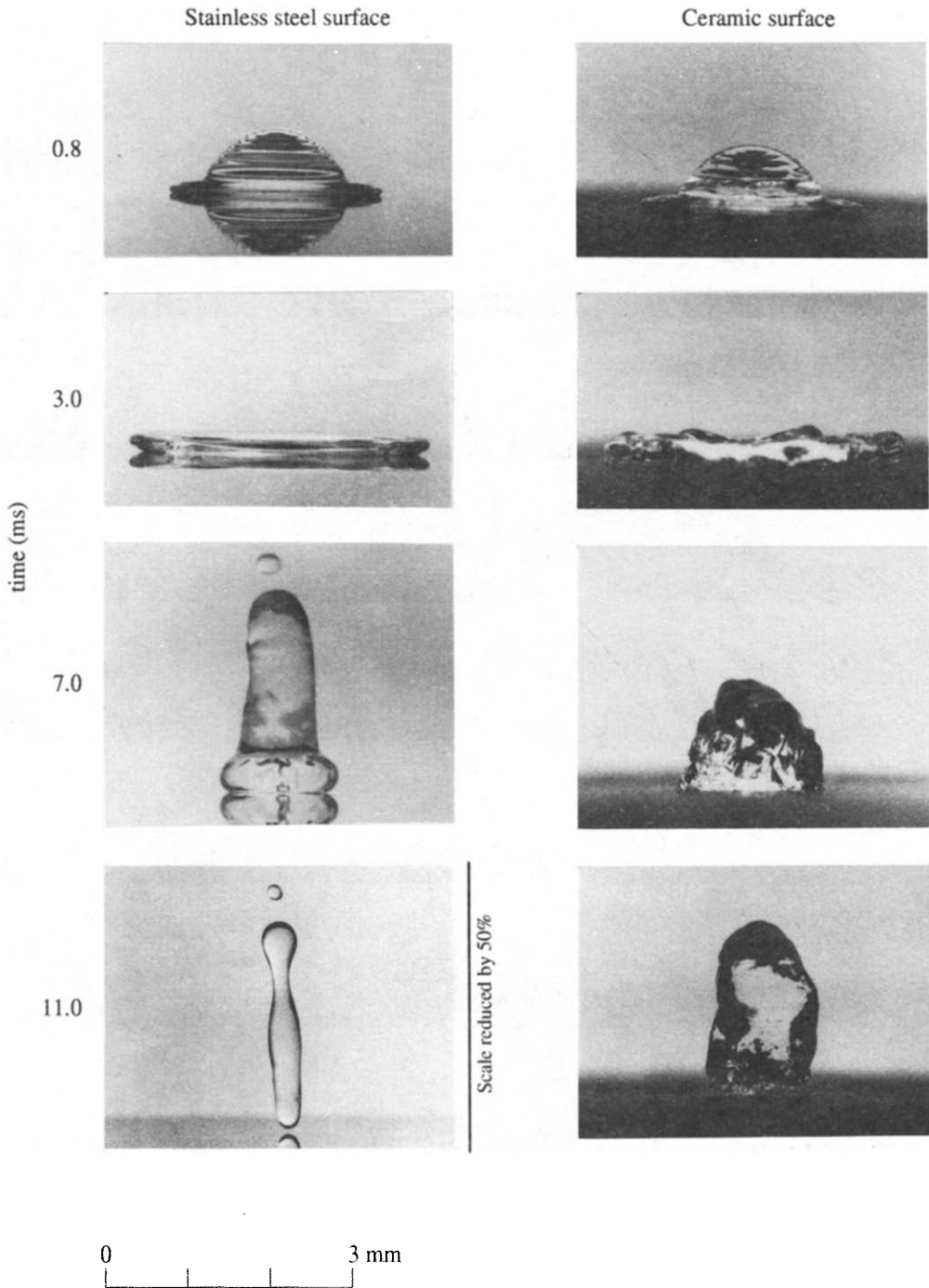


FIG. 6. Comparison of droplet impact dynamics on a ceramic surface with those on a stainless steel surface at a surface temperature $T_w = 200^\circ\text{C}$.

measurements of d were restricted only to the period of impact and first recoil at $T_w \geq T_{L,ss}$.

Measurement of β relies on the ability to discern the liquid front that spreads radially outward from the point of impact. When liquid penetrates into the surface, this front can be hidden from view and there-

fore appear smaller than it may really be (like an iceberg), especially if the porous surface promotes wetting (i.e. liquid being drawn up a piece of tissue paper). In the present study, β could only be measured by viewing the liquid on the air side of the ceramic surface.

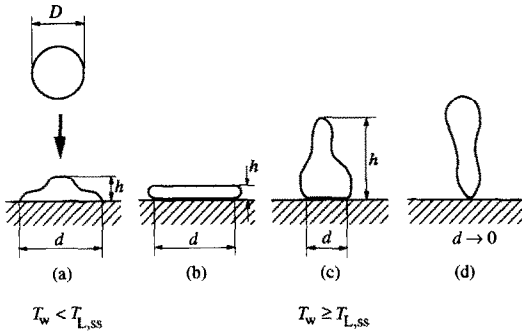


FIG. 7. Definition of d and h .

Figures 8 and 9 compare the evolution of β and ζ for the steel and ceramic surfaces. At the one temperature that ζ was measured (Fig. 8), room temperature, it appeared to be unaffected by surface porosity or roughness for the two surfaces studied. This fact is further illustrated in Fig. 3, which compares h for a droplet on a stainless steel and ceramic surface at room temperature. At this temperature, any differences between h for the two surfaces could not be observed as shown in Fig. 3. On the other hand, β was smaller on the ceramic surface at the early times after initial impact as shown in Fig. 8 at room temperature where the liquid wetted both surfaces. Though the differences between β for the two surfaces shown in Fig. 8 are rather small, they are nevertheless real. Figure 3 illustrates how such differences as shown in Fig. 8 appeared from the photographic prints. It is clear that $d_{ss} > d_p$ for the two droplets shown in Fig. 3. At higher temperatures (Fig. 9) differences in β for the two surfaces decreased in the early period of spreading during which time the wetted diameter on the two surfaces approached β_{max} . The spreading dynamics of the droplet would be expected to change when the surface is heated because of: (1) the vari-

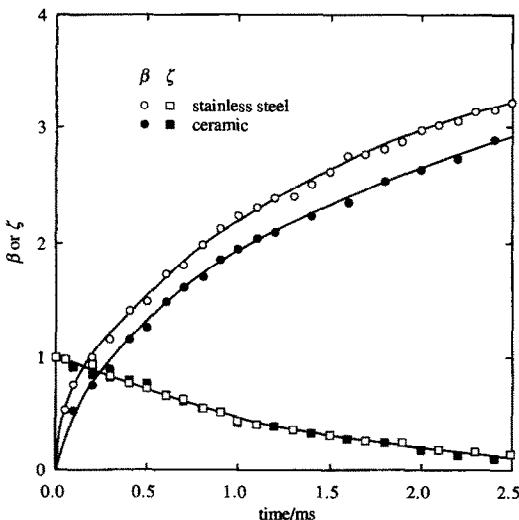


FIG. 8. Evolution of β and ζ during the impact of a droplet on both the stainless steel and ceramic surfaces for $T_w = 22^\circ\text{C}$.

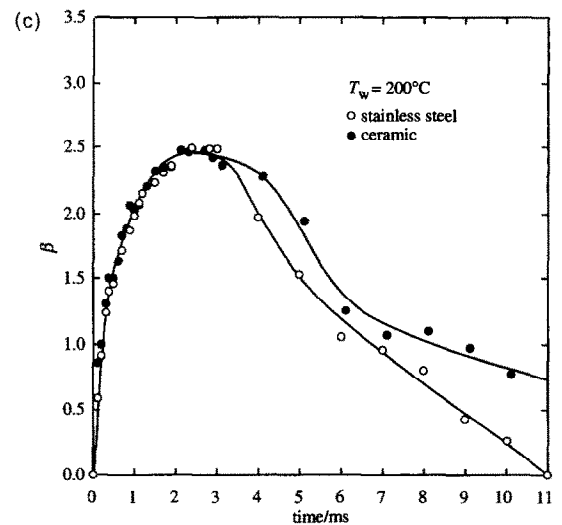
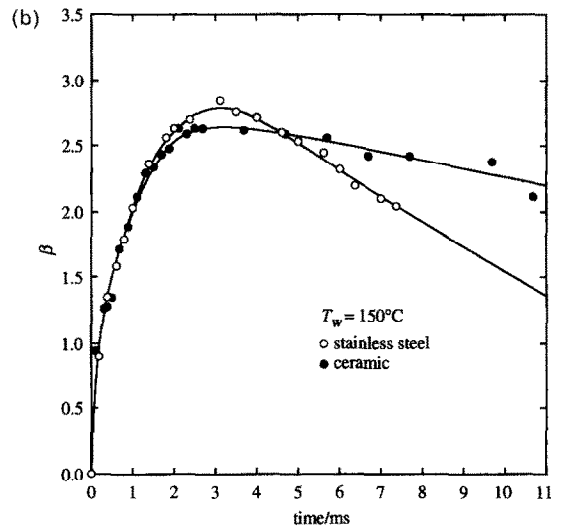
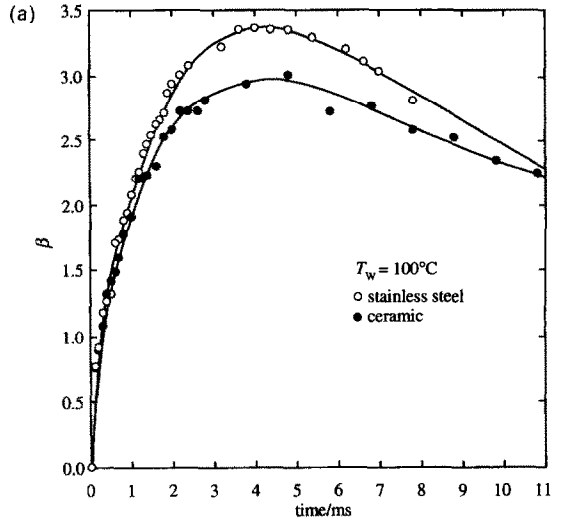


FIG. 9. Evolution of β during impact on both a stainless steel and ceramic surface with (a) $T_w = 100^\circ\text{C}$, (b) $T_w = 150^\circ\text{C}$, and (c) $T_w = 200^\circ\text{C}$.

ation with temperature of the liquid properties ρ , μ , and σ , and (2) formation of vapor at the liquid–solid interface when T_w is above the liquid boiling point (98.4°C). Variations in liquid properties have previously been shown to have a negligible effect on the magnitude of β , in connection with impact on a stainless steel surface [10]. It is conjectured, however, that as the surface temperature increases, greater amounts of vapor will be formed at the liquid–solid interface, thereby reducing the area of liquid–solid contact. Consequently, the roughness of the ceramic surface no longer retards the droplet spreading to the same extent that it did on an unheated surface, and $\beta_p \rightarrow \beta_{ss}$ as seen in Fig. 9.

The peak of β shown in Figs. 9(a)–(c) is a consequence of the droplet recoiling after impact (cf. Fig. 5). It can be shown through a simple order of magnitude analysis [10] that during the initial stages of impact the stagnation pressure in the drop, which drives the outward jetting of the liquid, is much larger than the restraining forces due to surface tension and viscosity (i.e. shear stress). As the droplet spreads out into a thin film the kinetic energy is, however, dissipated, stopping further spreading of the liquid. β then reaches a maximum value (β_{max}) after which it becomes smaller (cf. Figs. 5 and 6) as the droplet recoils from the surface or evaporates.

For a given T_w , the velocity of recoil of the tip of the liquid film ($d\beta/dt$) is also generally lower on the ceramic surface than on a stainless steel surface, possibly as a consequence of greater surface roughness of the ceramic surface and therefore greater wetting by the liquid. Once the droplet starts to recoil, however, the lower value of $d\beta/dt$ on the ceramic surface implies that β_p decreases at a lower rate than β_{ss} , so that we eventually get $\beta_p > \beta_{ss}$ (see Fig. 9(b), for $t > 5$ ms).

Because $T_{L,ss} \neq T_{L,p}$ a temperature range ($T_{L,p} - T_{L,ss}$) exists over which a droplet wets the porous surface but not the non-porous surface. The dynamics of the impact and recoil process will generally be different for the two surfaces over this temperature range (cf. Fig. 6). The shear stress acting on the liquid is greater for the porous surface than that for the non-porous surface because the liquid at the impermeable surface is separated from the solid by a thin vapor layer when $T_w \geq T_{L,ss}$. The droplet, floating on the vapor cushion, can deform more easily on the non-porous surface and thus it spreads out and recoils sooner than on the porous surface. At $T_w = 200$ C, the droplet recoils off the stainless steel surface (cf. Figs. 6 and 9(c)) and $\beta \rightarrow 0$ at $t \approx 11$ ms. For the porous surface, though, the droplet is not levitated, and β decreases at a slower rate as the liquid evaporates.

An analysis to predict the above results is complicated by the existence of moving boundaries of essentially unknown shapes which must be determined as a part of the solution. In addition, wetting, boiling, and the possibility of liquid penetrating into the surface (for a porous surface) further complicate the problem. In the present study, our attention was

directed toward determining a semi-quantitative formulation for β_{max} because of the importance of β_{max} in determining the effectiveness of cooling of a hot surface. The larger the wetted area, the more effective cooling will be. The approach taken is based on a global energy balance which equates the kinetic and surface energies before impact with these energies, and the energies associated with liquid penetration and viscous losses, after impact.

An overall energy balance on the droplet yields

$$E_{k1} + E_{s1} = E_{k2} + E_{s2} + W + E_p. \quad (3)$$

The terms in (3) that account for the energy associated with liquid penetration into the surface and wetting of the surface are E_p and E_{s1} , respectively. If liquid penetration is negligible, then $E_p = 0$ and (3) reduces to a previously presented result for an impermeable surface [10].

An expression for E_p is difficult to obtain. It should, though, be a function of the volume of liquid entering the surface. An estimate of this volume can be obtained directly from the two-dimensional photographic images when the droplet geometry is well defined before and during the impact process. For example, in Fig. 5, at $T_w = 100^\circ\text{C}$, the droplet shape is spherical with diameter D before impact ($t = 0$ s). After impact and at β_{max} the liquid shape is approximately that of a flattened circular disk (e.g. $t = 5$ ms). The difference in the two volumes is the volume of liquid that enters the surface.

To estimate the volume of liquid entering the ceramic surface, the volume of a droplet before and after impact was measured from the photographs. A stainless steel surface was first considered because the two volumes should be identical, with any small differences possibly being due to liquid evaporation. Assuming the two-dimensional image to be a volume of revolution at β_{max} (with a volume of approximately $\pi d_{max}^2 h/4$) resulted in volume estimates obtained from the photographs being about 3 to 4% lower after impact on the stainless steel surface than before impact. The volumes should, however, be equal because no liquid will penetrate the stainless steel surface. Two reasons for this difference in volume are: (1) a hydraulic jump occurs within the advancing liquid film which cannot be viewed, and hence corrections to the calculated volume cannot be made, because of the viewing angle of the camera ($\alpha = 0^\circ$ in Fig. 1); and (2) liquid evaporation.

On the ceramic surface, the difference in volume before and after impact was larger and ranged from 12 to 15%. This difference is too large to be explained solely by uncertainties in measurement and is believed to indicate liquid penetration into the surface (and to a lesser extent evaporation). It is an open question whether or not this volume change is significant enough to warrant inclusion in a simplified model. Certainly, to do so would greatly complicate the analyses. As a first approximation, we proceed on the assumption that volume losses into the surface of the

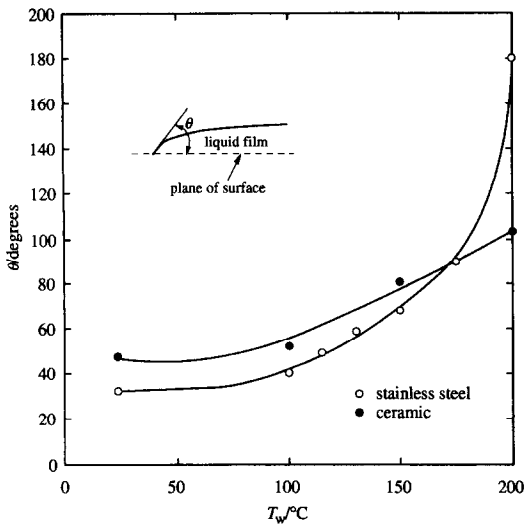


FIG. 10. Variation of θ with T_w for droplet spreading on both the stainless steel and ceramic surfaces.

order of 15% or less will not exert a strong effect on β_{\max} during the relatively short time period that β increases to β_{\max} . This time period is generally under 5 ms for an impact and evaporation process that spans several seconds (cf. Figs. 4 and 9). Hence, taking $E_p = 0$, it can be shown that (3) yields [10]

$$\frac{3}{2} \frac{We}{Re} \beta_{\max}^4 + (1 - \cos \theta) \beta_{\max}^2 - (\frac{1}{3} We + 4) \approx 0. \quad (4)$$

The influence of surface condition is carried entirely in the apparent contact angle as is the dependence of β_{\max} on T_w for constant Re and We . The temperature dependence of the apparent contact angle on the ceramic surface was measured from enlarged views of the tip of the advancing liquid film at the instant the wetted diameter reached d_{\max} . The results of these measurements are given in Fig. 10. The increase of θ

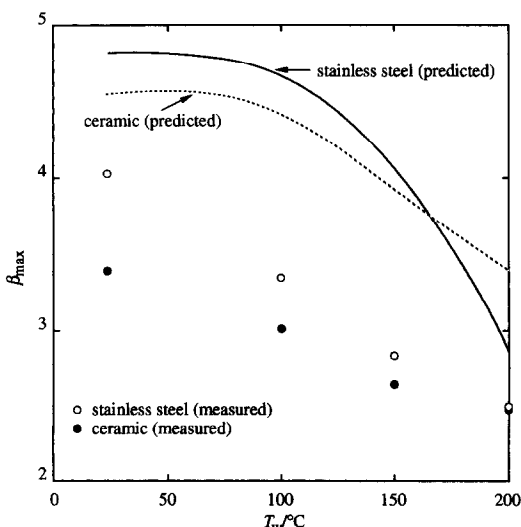


FIG. 11. Comparison of predicted (line) with observed (circles) variation of β_{\max} with T_w for droplet spreading on a stainless steel and ceramic surface.

with T_w for the stainless steel surface may be expected [15], and the data shown in Fig. 10 indicate that the same is true for the ceramic surface as well. For $T_w < 175^\circ\text{C}$, θ is greater on the ceramic surface than it is on the steel surface. At $T_w = 200^\circ\text{C}$, however, the droplet is in film boiling on the stainless steel surface so that there is no liquid–solid contact. The apparent contact angle is then assumed (defined) to be equal to 180° [18]. The droplet continues to wet the ceramic surface at this temperature, though, so that $\theta < 180^\circ$.

The curves shown in Fig. 11 are predicted variations of β_{\max} with wall temperature based on (4) assuming $Re = 2300$ and $We = 43$ which correspond to the present experimental conditions. The measured values are approximately 25% lower than the predictions of (4). Reasons for this discrepancy may be that the estimates of the energy losses during droplet deformation are too low and that the influence of liquid penetration (for the ceramic surface) is neglected. The analysis does, though, predict the general reduction in β_{\max} with increasing T_w noted experimentally. The convergence of the measured values of β_{\max} on the two surfaces as T_w increases also seems to be suggested by the simplified model.

Acknowledgements—The authors are grateful for the financial support provided by the National Science Foundation (grant No. CBT 8451075), the Semiconductor Research Corporation, and the Industry–Cornell University Alliance for Electronic Packaging.

REFERENCES

1. A. M. Worthington, On the forms assumed by drops of liquids falling vertically on a horizontal plate, *Proc. R. Soc. London* **25**, 261–271 (1877).
2. A. M. Worthington, A second paper on the forms assumed by drops of liquids falling vertically on a horizontal plate, *Proc. R. Soc. London* **25**, 498–503 (1877).
3. O. G. Engel, Waterdrop collisions with solid surfaces, *J. Res. Natn. Bur. Stand.* **54**, 281–298 (1955).
4. P. Savic and G. T. Boulton, The fluid flow associated with the impact of liquid drops with solid surfaces, Natn. Res. Council Canada, Report No. MT-26 (1955).
5. P. Savic, The cooling of a hot surface by drops boiling in contact with it, Natn. Res. Council Canada, Report No. MT-37 (1958).
6. L. H. J. Wachters and N. A. J. Westerling, The heat transfer from a hot wall to impinging water drops in the spheroidal state, *Chem. Engng Sci.* **21**, 1047–1056 (1966).
7. S. Toda, A study of mist cooling (2nd Report: Theory of mist cooling and its fundamental experiments), *Heat Transfer—Japanese Res.* **3**(1), 1–44 (1974).
8. F. Akao, K. Araki, S. Mori and A. Moriyama, Deformation behavior of a liquid droplet impinging onto hot metal surface, *Trans. Iron Steel Inst. Japan* **20**, 737–743 (1980).
9. S. Inada, Y. Miyasaka, K. Nishida and G. R. Chandratilleke, Transient temperature variation of a hot wall due to an impinging water drop—effect of subcooling of the water drop, *Proc. ASME-JSME Thermal Engineering Joint Conf.*, **1**, 173–182 (1983).
10. S. Chandra and C. T. Avedisian, On the collision of a droplet with a solid surface, *Proc. R. Soc. London A* **432**, 13–41 (1991).
11. C. T. Avedisian and J. Koplik, Leidenfrost boiling of

- methanol droplets on hot porous/ceramic surfaces, *Int. J. Heat Mass Transfer* **30**, 379–393 (1987).
12. T. Takano and K. Kobayasi, Study of vaporization of a single droplet impinging on a heated ceramic surface, *Japan Soc. Mech. Engng Ser. B* **53**(488), 1338–1343 (1987).
 13. S. Chandra, Droplet evaporation and combustion near a surface, Ph.D. Thesis, Cornell University (1990).
 14. K. J. Baumeister and F. F. Simon, Leidenfrost temperature—its correlation for liquid metals, cryogenes, hydrocarbons, and water, *J. Heat Transfer* **95**, 166–173 (1973).
 15. P. C. Wayner, A dimensionless number for the contact line evaporative heat sink, *J. Heat Transfer* **111**, 813–815 (1989).
 16. M. Fatehi and M. Kaviany, Analysis of levitation of saturated liquid droplets on permeable surfaces, *Int. J. Heat Mass Transfer* **33**, 983–994 (1990).
 17. C. Bonacina, S. Del Giudice and G. Comini, Dropwise evaporation, *J. Heat Transfer* **101**, 441–446 (1979).
 18. R. E. Ford and C. G. L. Furmidge, Impact and spreading of spray drops on foliar surfaces, *Wetting*, Soc. Chem. Industry Monograph No. 25, pp. 417–432 (1967).

OBSERVATION DE L'IMPACTION DE GOUTTELETTES SUR UNE SURFACE CERAMIQUE POREUSE

Résumé—On étudie expérimentalement les aspects dynamiques de l'impaction de gouttelettes sur une surface céramique poreuse. On photographie la déformation et l'étalement sur la surface. Les observations sont faites à la pression ambiante (0,10 MPa), à la température ambiante (ca. 22°C), pour un diamètre de goutte initial de 1,5 mm et pour un nombre de Weber fixé à 43. Le paramètre principal est la température de surface qui varie de 22°C à 200°C. Le liquide est le *n*-heptane. La vitesse d'étalement de la gouttelette sur la surface poreuse à 22°C est plus faible que sur une surface en acier inoxydable. On n'observe pas de transition à l'ébullition en film avec la surface poreuse à 200°C, alors que cela est observé sur une surface en acier inox. L'évolution de l'aire mouillée et de la vitesse d'étalement, pour une surface poreuse et pour une surface en inox, est indépendante de la température de la surface pendant le début de l'impaction. Cela résulte des faibles effets de la tension interfaciale et de la viscosité. La valeur maximale du diamètre de liquide étalé sur la surface est inférieur sur la surface céramique à celle sur l'acier inox pour la même température.

BEOBACHTUNG DES AUFSTREFFENS VON TRÖPFCHEN AUF EINER PORÖSEN KERAMIKOBERFLÄCHE

Zusammenfassung—Die dynamischen Vorgänge beim Auftreffen von Tröpfchen auf einer porösen Keramikoberfläche werden experimentell untersucht. Stroboskopische Aufnahmetechnik wird eingesetzt, um die seitliche Verformung und Ausbreitung auf der Oberfläche festzuhalten. Die Untersuchungen wurden bei Umgebungsdruck (101 MPa), Umgebungstemperatur (ca. 22°C), einem anfänglichen Tropfendurchmesser von 1,5 mm und einer Weber-Zahl von 43 durchgeführt. Der wichtigste Parameter ist die Oberflächentemperatur, die zwischen 22 und 200°C variiert wurde. Als Flüssigkeit wird *n*-Heptan verwendet. Die Messung ergab, daß die Ausbreitungsgeschwindigkeit eines Tröpfchens auf einer porösen Oberfläche mit 22°C kleiner ist als die auf einer Stahloberfläche. Bei der 200°C heißen porösen Oberfläche konnte kein Übergang zum Filmsieden beobachtet werden, wie dies etwa bei Stahl der Fall ist. Die Entwicklung der benetzten Fläche und der Ausbreitungsgeschwindigkeit erweist sich in einer ersten Phase als unabhängig von der Oberflächentemperatur; dies gilt sowohl für die poröse als auch für die glatte Oberfläche. Dieses Ergebnis wird den vernachlässigbaren Einflüssen von Oberflächenspannung und Viskosität zugeschrieben. Der maximale Ausbreitungsdurchmesser der Flüssigkeit auf der Oberfläche ist bei gleicher Temperatur für Keramik kleiner als für Stahl.

НАБЛЮДЕНИЯ ЗА СОУДАРЕНИЕМ КАПЛИ С КЕРАМИЧЕСКОЙ ПОРИСТОЙ ПОВЕРХНОСТЬЮ

Аннотация—Экспериментально исследовались динамические аспекты соударения капли с пористой керамической поверхностью. Для регистрации деформации капли и ее растекания на поверхности использовалось однокадровое фотографирование со вспышкой. Наблюдения проводились при фиксированных давлении (101 МПа) и температуре (около 22°C) окружающей среды, начальном диаметре капли (1,5 мм) и числе Вебера для соударения (43). Основным параметром была температура поверхности, которая изменялась от 22 до 200°C. В качестве рабочей жидкости использовался *n*-гептан. Измерения показали, что скорость растекания капли на пористой поверхности при 22°C ниже, чем на поверхности из нержавеющей стали. В отличие от последней, для пористой поверхности переход к пленочному течению при температуре поверхности 200°C не наблюдался. Найдено, что эволюция смачиваемой области и скорость растекания капли как на пористой поверхности, так и на поверхности из нержавеющей стали не зависят от температуры поверхности на раннем этапе соударения. Этот результат объясняется пренебрежимо малым поверхностным натяжением и вязкостными эффектами. Обнаружено, что максимальное значение диаметра растекающейся капли жидкости на керамической поверхности ниже, чем на поверхности из нержавеющей стали при одинаковой температуре.